COUPLING OF SOIL-STRUCTURE INTERACTION AND NONLINEAR RESPONSE OF LIQUEFIABLE SOILS

S. Montoya-Noguera[1] , F. Lopez-Caballero[2]

[1] *PhD, silvana.montoya-noguera@centralesupelec.fr*
[2] *Senior researcher, fernando.lopez-caballero@centralesupelec.fr*
[1,2]*MSSMat CNRS UMR 8579 lab, CentraleSupélec, Paris-Saclay Univ., Châtenay-Malabry, France*

Abstract

The current seismic design philosophy is based on nonlinear behavior of structures where the foundation soil is often simplified by a modification of the input acceleration depending on the expected site effects. When taking into account nonlinear soil behavior, the isolation of structure and soil is no longer valid and soil-structure interaction has to be taken into account. Additionally, when the soil is loose and saturated, more robust models that take into account pore pressure generation are needed. Findings presented in this work illustrate the importance of accounting for both added soil nonlinearity due to seismic liquefaction and for soil-structure interaction.

Some models can account for the nonlinear behavior of soils neglecting the effect of pore-pressure distribution and migration, as if the soil was fully drained. However, in most cases, this condition is not valid and there is a need for nonlinear models capable of taking into account the coupling of excess pore pressure (Δp_w) and soil deformation (CPD). In order to highlight the importance of these models, a CPD analysis is compared to a mechanical-equivalent fully drained decoupled (DPD) analysis of a 2D finite element model subjected to a wide range of earthquake motions. Additionally, to assess the effect of CPD combined with SSI, three systems were tested: two nonlinear structures and a model without a structure to use as reference. The differences between the analyses on different engineering demand parameters are evaluated.

The effect of the structure on the soil can be observed on the slightly increase on pore-pressure generation throughout the deposit and on the differences in the acceleration amplification at surface, especially when SSI effects are important. With respect to the structure, its coseismic relative settlement with respect to free field can be half if DPD is used. Additionally, concerning the maximum inter-story-drift (ISD), the DPD analysis will underestimate the response for 75% of the motions tested. The combined effect of input ground motion, nonlinear soil and nonlinear structure behavior makes the task of predicting the seismic performance very difficult. Hence for more realistic models both SSI and CPD effects should be taken into account.

Keywords: Soil-structure interaction; soil nonlinearity; liquefaction

Introduction

Usually in the earthquake engineering practice, the effects of dynamic soil-structure interaction (SSI) and of the nonlinear soil behavior are either neglected or simplified. Moreover, when these effects are taken into account, in most cases the nonlinear soil response is modeled without including the pore-water behavior (i.e. total stress approach). In contrast, coupled effective stress analysis allows the modeling of the generation, redistribution and eventual dissipation of excess pore pressure (Δp_w) during and after earthquake shaking.

Recent studies [1,2,3] have evaluated the effects of coupling Δp_w and deformation on the soil behavior (CPD). In these studies, focus was given mainly to the effects on the ground motion amplitude and frequency content. All of these analyses have been performed in free-field 1D conditions. However, to the best knowledge of authors, no study has been published that accounts for the effects of coupling Δp_w and soil deformation on the performance of structures founded on cohesionless soils. While PGA and other intensity measures can be lower with CPD analysis in 1D soil profiles, results could differ with the added effect of the 2D migration and distribution of pore pressure and of the structure's load and seismic performance.

This paper concerns the assessment of the CPD effect on the performance of a structure founded on liquefiable soil. For this purpose a 2D fully nonlinear soil - structure model is subjected to a variety of unscaled earthquake signals. A fully coupled analysis is used to represent the soil behavior. With the same model, a fully drained (or decoupled – DPD) analysis is also performed. The combined effect of SSI and CPD on several parameters of the soil, the structure and the motion is studied. It should be mentioned that this paper is part of a larger study presented in other publications [3,4].

1. Numerical model

Two soil-structure models are considered in this work. They consist of reinforced concrete (RC) buildings with a shallow rigid foundation, standing on saturated cohesionless soil. A schema of the models is shown in Fig. 1.

(a)   (b)
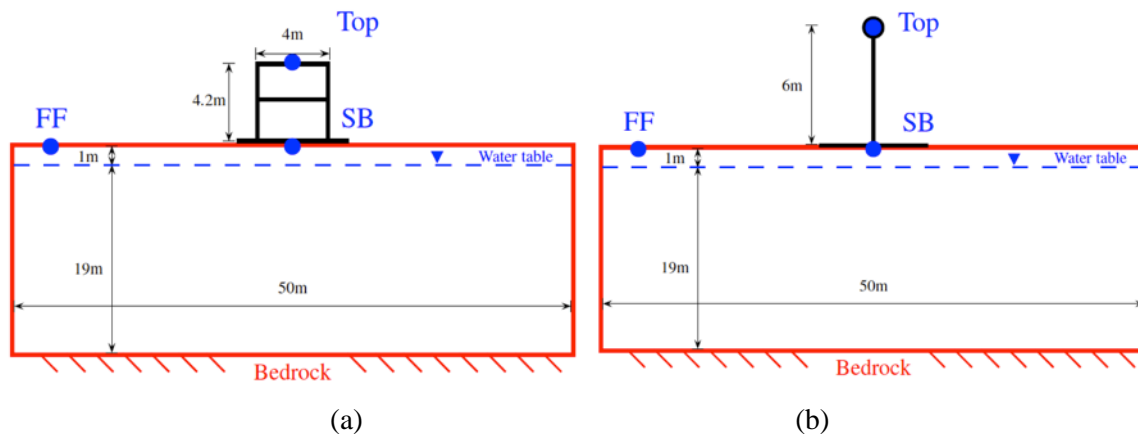
Fig. 1. Schema of the numerical model for a) B01 and b) T040. The structure's Top, the structure's base (SB) and the free-field (FF) will be used for calculations.

One structure is modeled as an RC frame of one span and two stories and the other is a single-degree-of-freedom (SDOF). The dynamic performance of the structures is different as they have different height, weight and predominant periods. Both structures lay on a rigid foundation. All structural elements are elastoplastic. Concerning the soil model, a 50m wide and 20m thick deposit of loose-to-medium sand is overlaying an elastic bedrock. The maximum shear modulus (G_{max}) profile increases with depth and the equivalent shear wave velocity of the first 20m (V_{s20}) is 200m/s. The fundamental elastic period of the soil profile is 0.38s. An elastoplastic multi-mechanism model is used to represent the soil behavior. Under the deposit, the engineering bedrock is considered deformable and it is representing a half-space medium with an isotropic linear elastic

behavior and a shear wave velocity (V_s) equal to 550m/s. The ground water table is located 1m below the surface.

1.1 Finite Element Model

As the soil is assumed to be horizontally homogeneous, a 2D finite element computation with plane-strain assumption was performed. The finite element code GEFDyn [5] was used. The saturated soil was modeled using quadrilateral isoparametric elements with eight nodes for both solid displacements and fluid pressures. The element size is 1m wide by 0.5m thick.

1.1.1 Coupled and Decoupled dynamic approach

Modaressi [6] introduced the coupling of pore pressure and soil deformation on GEFDyn. It follows the simplified Biot's generalized consolidation theory [7] known as $\underline{u}$ - p_w formulation. This formulation consists of neglecting fluid acceleration and its convective terms so that the unknown variables remain the displacement of the solid ($\underline{u}$) and the pore water pressure (p_w). The behavior of the solid skeleton is derived assuming the principle of effective stress as proposed by Terzaghi [8]. The momentum and equilibrium conservation equations take into account the total unit mass, the permeability tensor and the compressibility parameter. In this study, the decoupled analysis consists in keeping the same inertial effects while no excess pore pressure is generated. Hence it reproduces a fully drained condition where the soil stiffness degradation depends only on the shear strain.

1.1.2 Boundary conditions

Concerning boundary conditions, as the signal propagation is 1D and the response of an infinite semi-space is modeled, equivalent boundaries have been imposed on the lateral nodes [9]. For the bedrock's boundary condition, paraxial elements simulating "deformable unbounded elastic bedrock" have been used [10]. These elements efficiently evacuate diffracting waves in a local domain while the vertically incident shear waves, defined at the outcropping bedrock, are introduced into the base of the model after deconvolution. Thus, the obtained movement at the bedrock is composed of both incident and reflected waves. For the CPD analysis, during the initial gravity consolidation phase a hydrostatic potential develops from the groundwater table downward. Then, during the dynamic loading, p_w is allowed to change below this level as a result of soil contraction and dilation due to shear strains. For the bedrock's boundary, the pore pressure conditions are assumed to be impervious. Therefore, no flux occurs across the interface boundary between the studied domain and the underlying semi-infinite space.

1.2 Soil constitutive behavior

The elastoplastic multi-mechanism model used is the ECP model, developed at École Centrale Paris [11]. It uses a Coulomb type failure criterion and follows the critical-state concept. It can take into account a large range of deformations. For the cyclic behavior it uses a kinematic hardening, which relies on the state variables at the last load reversal. For a complete description of the model refer to Aubry et al. [12]; Hujeux [13]; and Lopez-Caballero and Modaressi-Farahmand-Razavi [14] among others. The soil model parameters used in this study were determined with the procedure defined by Lopez-Caballero et al. [15] and can be found in Montoya-Noguera and Lopez-Caballero [3].

Drained cyclic shear tests are simulated in order to show the cyclic behavior of the soils used. Results for the LMS are shown in Fig. 2. The other soil has similar curves and they are not shown here for the sake of brevity. As a reference, the curves given by Darendeli [16] for the same confinement pressures, IP = 0 %, OCR = 1, f = 1 Hz and N = 10 cycles are also shown in the figure. The obtained shear degradation curves (G/G_{max} - γ) match relatively well. Whereas for the damping (D), it can be seen an overestimation for large strains, which is a known limitation of this type of models.
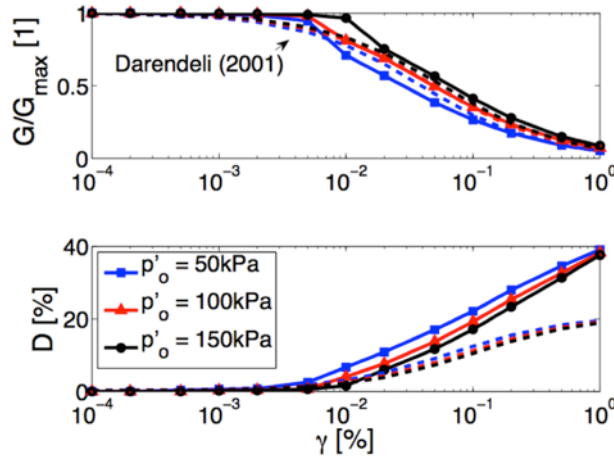
Fig. 2. Normalized shear degradation and damping evolution with shear strain for different confinement pressures. Darendeli [16] curves are given as reference.

1.3 Structure's model

Two models were used in order to analyze the effect of the coupling pore-pressure and soil deformation for different predominant periods. The structures used will be called B01 and T040 and are reinforced concrete buildings with different size, weight and stiffness. The former is a large-scale, one-span, two-story frame model proposed by Vechio and Emara [17]. In contrast, T040 is a single-degree-of-freedom (SDOF) equivalent to a one-span, three-story building. Saez et al. [18] developed both model. These structures are used in this study to highlight the effects of the soil behavior in the structure's performance near resonance. The main characteristics of both structures are shown in Table 1. The structure's foundation is modeled as a rigid block of 10cm thick and 6m wide. Between the foundation and the soil, interface elements are used to allow relative movement of the structure with respect to the soil, in order to avoid the traction effect. These elements follow a Coulomb-type plastic criterion.

Table 1. Structures' main characteristics

Characteristic	B01	T040
Total height [m]	4.2	6
Width [m]	4	N/A
Mass [ton]	45	120
Fundamental fixed-base period T_0 [s]	0.24	0.40

The building's weight affects the stress state as well as the volumetric deformations; hence it affects the "distance to reach the critical state". This distance is defined in the ECP model as the degree of mobilized friction (r_k), as follows:

$$r_k = \frac{q_k}{p'_k \cdot F_k \cdot \sin \phi'_{pp}} \tag{1}$$

where p'_k is the mean stress, q_k is the deviatoric stress, ϕ'_{pp} is the friction angle at the critical state and F_k is the isotropic hardening associated with the volumetric plastic strain (ε_v^p). Thus, the effect of the inertial load on the soil behavior is seen on the differences in r_k, which is shown in Fig. 3 for both structures.
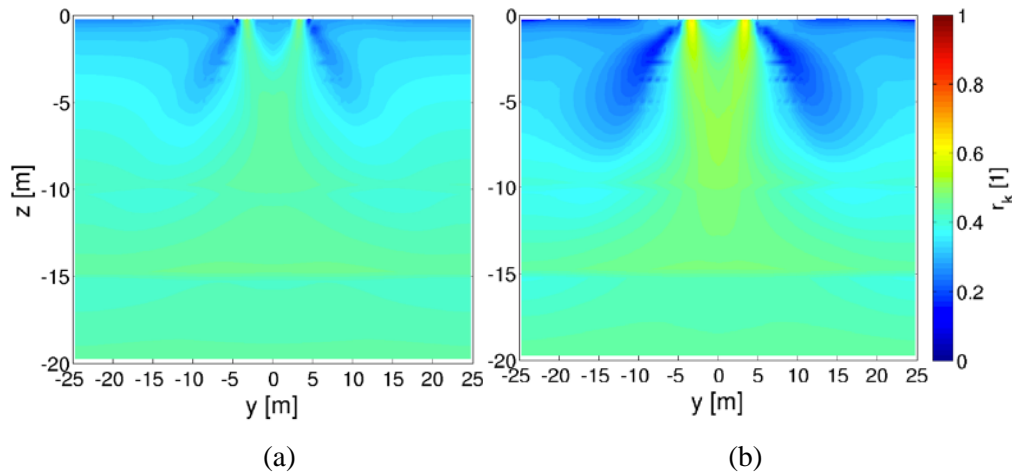
Fig. 3. Degree of mobilized friction (r_k) before shaking for a) B01 and b) T040

As r_k reachs unity, the soil approaches perfect plasticity. r_k is related to the inverse of the factor of safety (FS); however, as it is below unity, the soil has not arrived to failure. Evidently, the soil under the building presents higher values. Additionally, as T040 is heavier, r_k values are higher. The maximum value found is 0.6, hence FS is equal to $1/0.6 \approx 1.7$. As the coefficient of earth pressure at rest (k_0) also increases with the building load, the surrounding soil is stiffened but without the effect of the shear stress. Thus the soil on this region will present higher liquefaction resistance.

Concerning the initial state, a scaled motion with very low amplitude (i.e. PHA~1×10^{-5}g) was used to evaluate the pseudo-elastic behavior of both soil and structure. Fig. 4 shows the transfer functions (|TF|) with fixed base and with soil-structure interaction (SSI) effects (top/FF). In addition, |TF| of the soil deposit (FF/bedrock) is also shown. Firstly, it is interesting to note that, even if B01 has two stories, only one resonant frequency (or mode) is observed - as the other one is above 15Hz. Hence both structures behave as SDOFs. The SSI effects consist of a shift to lower frequencies due to the soil's flexibility and a deamplification due to the soil's material and radiation damping [19]. As expected, B01 being more rigid presents a higher interaction with the soil; hence, the deamplification and the frequency shift are greater. The relative position of the fundamental frequency of the soil with respect to the structure and the frequency content of the input motion is very important for the inelastic dynamic SSI effects [18]. Thus, as T040 main frequency is lower than that of the soil, higher SSI effects are expected when nonlinear soil degradation causes a shift of the soil frequency to lower values.

1.4 Input motions

Ninety unscaled records were chosen from the Pacific Earthquake Engineering Research Center (PEER) database. The signals used were recorded near the source - with a site-to-source distance below 70km- and in dense soil conditions - i.e. 30m averaged shear-wave velocity (V_{s30}) above 600m/s. These signals are supposed to have minimal noise and are appropriate for an outcropping bedrock condition. The events range between 6.2 and 7.7 in moment magnitude.
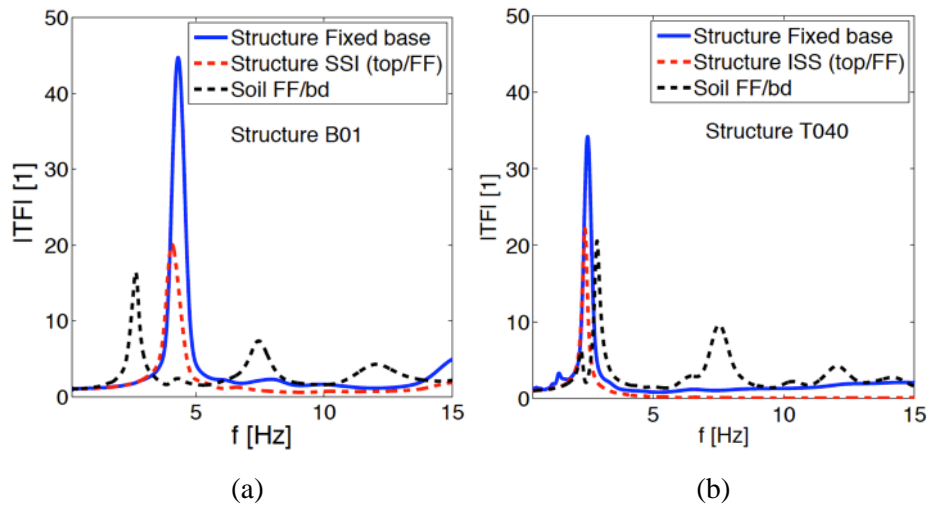
Fig. 4. Transfer function of the free field and the structure for a) B01 and b) T040

The statistics of some earthquake parameters calculated at outcropping conditions are shown in Table 2. These parameters are peak horizontal acceleration (PHA), peak ground velocity (PGV), Arias intensity (I_A) and significant duration ($D_{5\,95}$). The coefficient of variation (CV) is high for all parameters and it is about 130% for I_A. The latter is of great importance given that after the sensitivity analysis performed by Lopez-Caballero and Modaressi [14], it was proved to be the most influential input variable on the average liquefaction developed on the upper 10m of the deposit, known as $Q_{H=10}$. Fig. 5 shows the acceleration response spectra of the motions; accelerations were filtered to 20Hz and the spectral amplitude has a 5% structural damping. Similarly, a great variation is presented on the response spectra.

Table 2. Statistics of some earthquake parameters.

Parameter	Range	Mean	CV [%]	Median
PHA [g]	0.03 – 1.16	0.34	85	0.26
PGV [cm/s]	3.15 - 121	30.52	92	21.80
I_A [m/s]	0.02 – 11.53	2.17	136	0.64
$D_{5\,95}$ [s]	4.12 – 36.47	17.04	58	14.59
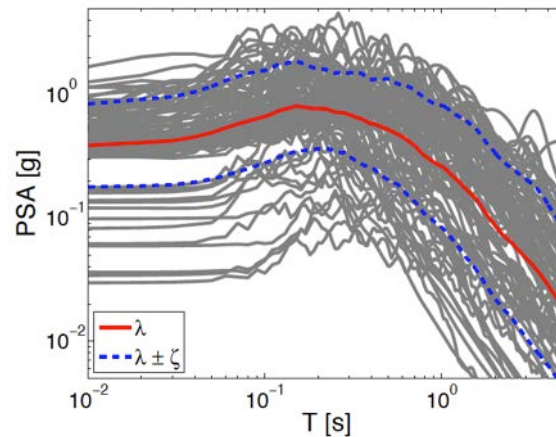
Fig. 5. Response spectra of acceleration for the outcropping motions. The geometric mean and +/- standard deviation are shown in red and blue, respectively.

2. Analysis and Results

The effect of coupling pore pressure and soil deformations on a soil-structure model is highly complex and will affect several aspects of the response. One important issue is the effect of the building load on the soil behavior. As seen in Fig. 3, the effective stress state before shaking (σ_0') is affected by the building. Additionally, with a CPD analysis, the excess pore pressure (Δp_w) evolves differently in the deposit. Fig. 6 shows the liquefaction ratio ($r_u = \Delta p_w / \sigma_0'$) at the end of shaking with the same motion but different structures. It is interesting to note that although the same input motion is used, the behavior of the deposit can be strongly affected by the structure. For T040, as the soil under the structure is stiffened, liquefaction is not presented there; however, around this area and because of the differences in the degree of mobilized friction, high r_u values appear beyond the structure's influence.

(a)   (b)
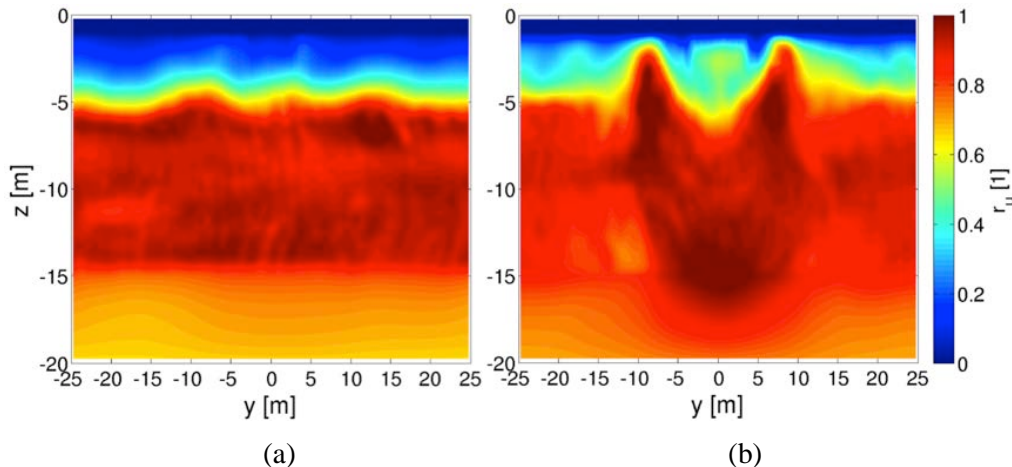
Fig. 6. Liquefaction ratio at the end of shaking (r_u) for a) B01 and b) T040

The triggering of liquefaction depends on the soil behavior and the motion characteristics. Hence different input motions will produce an increase in pore pressure generation in different zones on the soil deposit. In order to quantify it, the liquefaction index (Q) firstly introduced in 1D by Shinozuka and Ohtomo [20] will be used. It can be extended to a 2D model as:

$$Q_{H \cdot L} = \frac{1}{H \cdot L} \int_0^H \int_0^L r_u(y, z) \mathrm{d}y \mathrm{d}z \qquad (2)$$

where H is the thickness and L is the length evaluated. When $Q_{H \cdot L}$ is equal to unity, it means that liquefaction is present throughout the area $H \cdot L$; thus it gives information of the liquefaction ratio as well as the total liquefied zone. In Fig. 7, two $H \cdot L$ areas are tested and the results of a 2D model without a structure are compared to the models with one –i.e. taking into account the SSI effect.
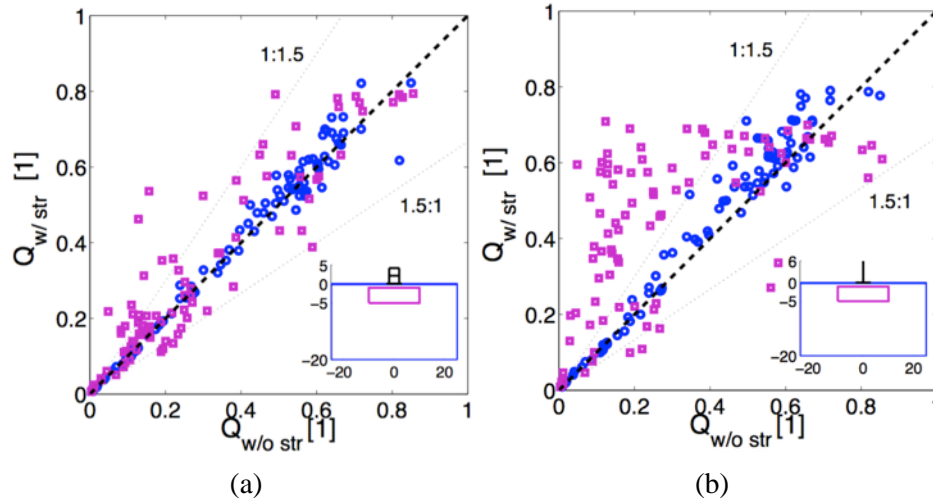
Fig. 7. SSI effect on the liquefaction index ($Q_{H \cdot L}$) for a) B01 and b) T040. The colors correspond to the size of the $H \cdot L$ area depicted on the schema.

It can be noted that when $Q_{H \cdot L}$ uses the total size of the Finite Element Model, called Q_{FEM} and colored in blue, there is only a slight increase when the structure is present, most notably for T040. Hence for these cases, SSI is prejudicial for liquefaction triggering throughout the model. In contrast, for $Q_{H \cdot L}$ evaluated at the $4 \cdot 20$ box under the structure, Q_{box} the effect of SSI on liquefaction varies greatly. Other sizes were evaluated and results slightly change; but for the sake of brevity only results for this area are shown. This area was selected according to the width of the foundation and by engineering recommendations for liquefaction mitigation given by Mitchell et al. [21]. Q_{box} evidences more dispersion and in most cases, more liquefaction will appear when the structure is present, specially with T040. For example, in one case, with T040 the deposit presented five times higher Q_{box} than without structure. With B01 it seems that for high liquefaction levels the results with and without structure are closer, which means that less SSI effect is present. In contrast, for T040 a plateau at about 0.7 is found for the Q_{box} values evaluated with SSI, which can be related to the pore pressure dissipation and the fact that these values are measured at the end of shaking and not at their maximum. For further details on this analysis please refer to Montoya-Noguera [4]. In order to have a better relation with the motions energy and less influence on the structure used, the area of the entire finite element model (FEM) will be taken into account hereafter.

2.1 On the surface acceleration

One of the known liquefaction consequences is the deamplification of energy at surface due to damping and energy dissipation. However, the structure's load and inertial force affects the acceleration on surface. To analyze it, Fig. 8 compares the PGA values at the structure's base (SB) with those evaluated near the lateral boundary i.e. in free-field (FF) for both structures and with both analysis. In general, the results at SB are higher than those at FF. With refer to the coupling of pore pressure and deformation, all PGA values are reduced with CPD analysis; however, the difference is greater for PGA at the base of B01 structure. For this case, it seems that the SSI effects are more important hence when pore pressure is not modeled the response could be highly

overestimated. In other words, it is considered that the modeling of liquefaction will have beneficial effects on the acceleration at surface.
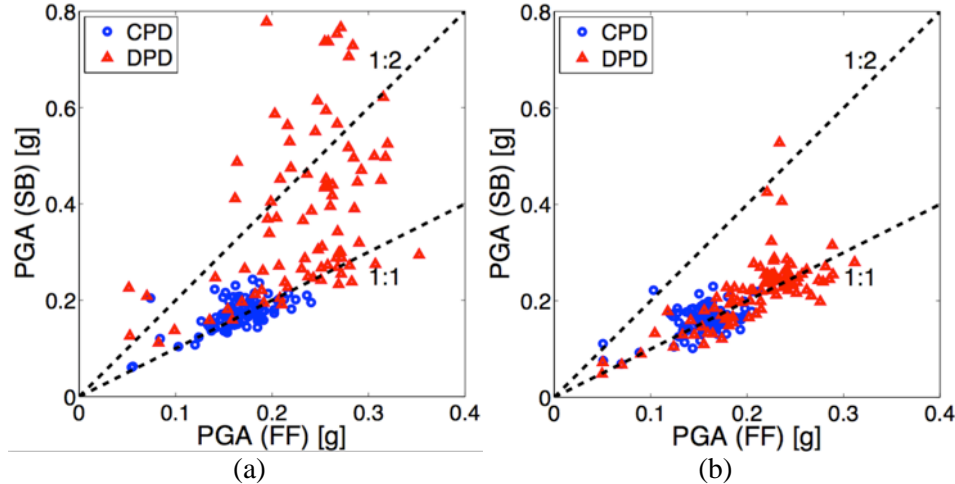
Fig. 8. Maximum acceleration at the structure's base compared to the free field for: a) B01 and b) T040.

2.2 On the structure's settlement

The soil-structure interaction also affects the vertical displacement (u_z) on the model. Evidently, u_z at the structure's base is higher due to the additional load. Furthermore, due to the pore-pressure migration in CPD analysis, u_z at free field varies. Thus, in order to assess the combined effect of CPD and SSI, the settlement of the structure is given relative to FF (i.e. $|u_z| = |u_{z\,SB} - u_{z\,FF}|$). In Fig. 9 the u_z evolution with time at SB and FF is shown for both analyses and both structures for one motion tested. It can be seen that the results vary greatly depending on the analysis type, the position in the model and the structure used. It is interesting that for the results at FF with the CPD analysis and T040, the values are positive at the end of shaking, which describes the apparition of a heave at the sides of the structure. Moreover, the evolution of this heave is also related at the time series of u_z under the structure, which start to diverge after the PHA instant. It is therefore evident the pore-pressure migration from below the structure to the surrounding soil. Hence at the end of shaking $|u_z|$ is bigger for the CPD analysis. However, with the B01 structure, this migration is not clearly shown at FF and for this case, the CPD $|u_z|$ is slightly lower than the DPD one.

(a)   (b)
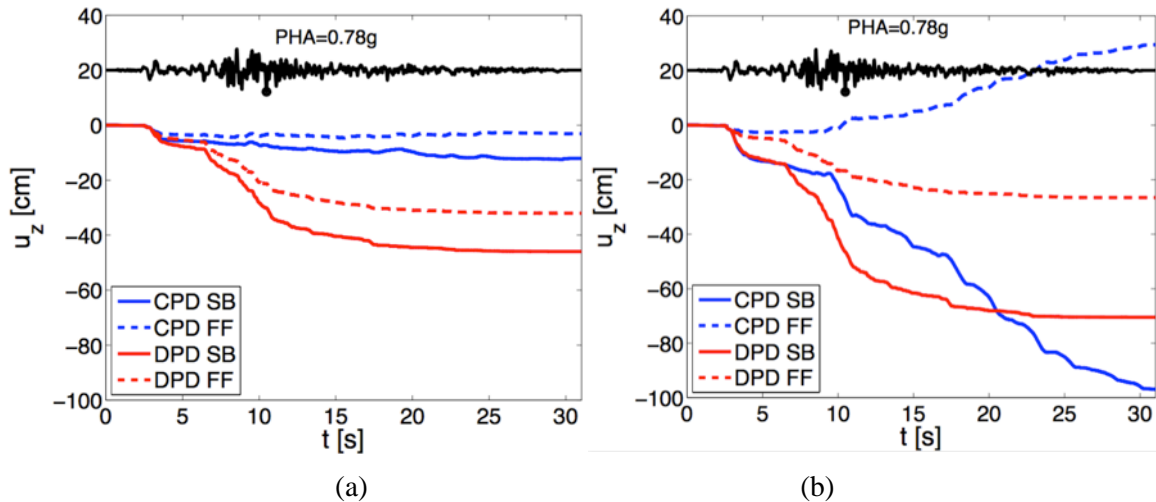
Fig. 9. Time history evolution of the vertical displacement (u_z) at the structure's base (SB) and at free-field (FF) with CPD and DPD analyses for: a) B01 and b) T040. The outcropping motion is shown in black as reference.

A comparison of $|u_z|$ at the end of shaking with CPD and DPD analyses is presented in Fig. 10 for each structure. Taking into account the effect of coupling in most cases will result in higher values, except for some cases of low levels of liquefaction and with the B01 structure. It appears that the differences between the analyses increase with the liquefaction level and the settlement. Note that for some cases, the CPD results are about 10 times greater than the DPD ones. Hence, once more, without coupling pore pressure and deformation results will be unconservative or even dangerous for the structure.

(a) *(b)*
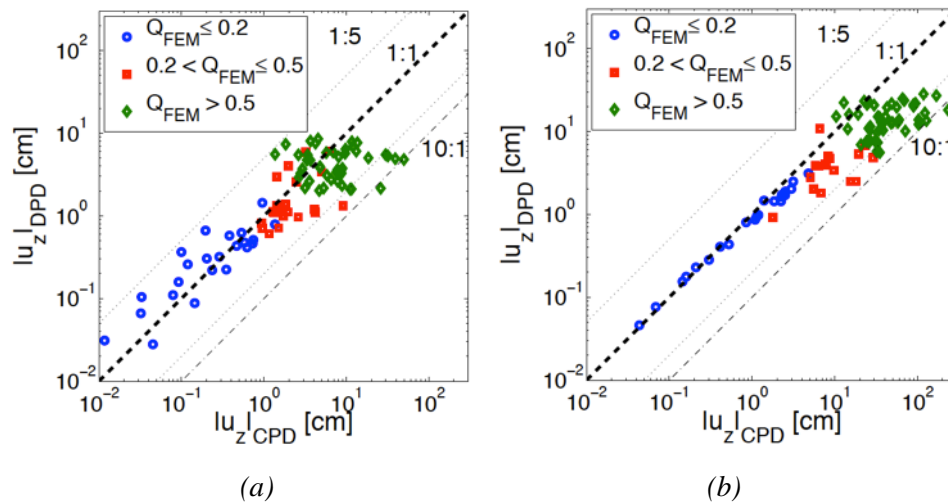
Fig. 10. Comparison of CPD and DPD results for the structure's settlement with a) B01 and b) T040 structures

2.3 On the structure's seismic demand

Regarding the seismic demand on the structure, the comparison of CPD and DPD results for the maximum inter-story drift (ISD) is shown in Fig. 11. This parameter is appropriate to analyze the effect on the drift in structures with different height as it normalizes the maximum horizontal displacement evaluated at each level by its corresponding height. In this case, the two structures present very different results. For B01, the CPD values are greater than the DPD ones for almost all cases; while for T040, it is the contrary. This is due to the higher effect of SSI presented with B01, as shown in Fig. 4, compared to the coupling effect. But when the liquefaction level increases, the latter is more important as the soil will attenuate the motion and the structure drift with CPD will be reduced. Concerning T040, the values with the DPD analysis are more than doubled when Q_{FEM} is above 0.5 and some are even four times greater. Additionally, a high dispersion is evidenced for these values. For models where structure's nonlinearity is taken into account but there is no coupling of Δp_w with soil deformation, the response could be largely overestimated. This would lead to a conservative design. In contrast, when SSI effects are important, the lack of coupling of Δp_w will lead to an unconservative or prejudicial conception.
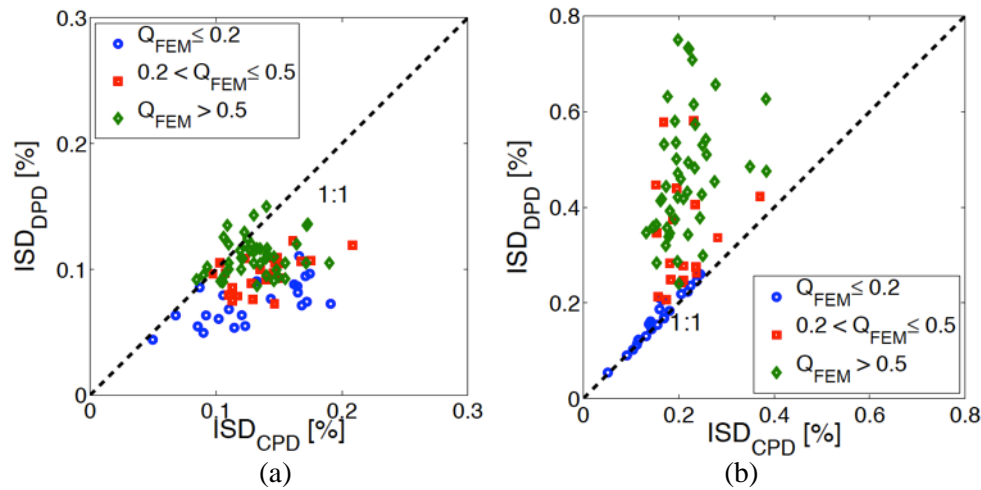
Fig. 11. Comparison of CPD and DPD result for the maximum interstory drift with a) B01 and b) T040.

3. Conclusions

A finite element analysis was used to investigate the effect of coupling excess pore pressure and soil deformation on a soil-structure model. Two mechanically equivalent analyses were performed with 90 unscaled earthquake motions: one taking into account coupling (CPD) and one fully-drained (DPD). The same effective-stress model was used for the calculations and the initial elastic behavior was proved to be identical. The present study aimed to highlight the importance of accurately model liquefiable soils in order to improve performance-based earthquake engineering (PBEE).

One of the main findings of this study is that when models are fully drained, and SSI effects are present, the relative settlement of the structure is underestimated for most motions with both structures tested. Even if in free-field (FF), DPD analysis presents higher vertical displacements, the structure's weight affects the soil behavior and hence the structure's settlement with respect to FF is in general underestimated with DPD models. Additionally, if the SSI effects are significant, i.e. when the predominant period of the structure is near to that of the soil, the maximum ISD is consistently underestimated by the DPD analysis. In this regard, the use of DPD models will not be recommended for a PBEE design. Two main effects are involved in this analysis: the coupling of pore pressure and soil deformation and the interactions between the soil deposit and the structure. These can be beneficial or detrimental for different EDPs but the analysis should include both, as it seems that the complex relation between them will vary for each motion, soil and structure tested.

The relation of both SSI and CPD effects was shown to be highly complex. Thus, the effects of CPD could be further evaluated for other soil deposits and other structures in order to increase the reliability of the results. Furthermore, some challenges are still to be acknowledged. To enrich the structural modeling, the evaluation of damage and failure could be included. Additionally, the effect of spatial variability and basin edge surface waves could also enhance liquefaction and should also be included. This work builds a framework to analyze more realistic and complex systems yet some challenges are still to be acknowledged.

4. Acknowledgements

5. References

[1]   Hartvigsen (2007): *Influence of pore pressures in liquefiable soils on elastic response spectra.* Master's thesis, University of Washington, Seattle.

[2]   N. Yoshida (2013): Applicability of total stress seismic ground response analysis under large earthquakes. In *COMPDYN2013: 4th ECCOMAS Thematic Conference on Computational methods in structural Dynamics and earthquake engineering*, id 13, Kos Island, Greece, June.

[3]   S. Montoya-Noguera and F. Lopez-Caballero (2016): Effect of coupling excess pore pressure and deformation on nonlinear seismic soil response. *Acta Geotechnica*, 11(1):191– 207, February.

[4]   S. Montoya-Noguera (2016): *Assessment and mitigation of liquefaction seismic risk: Numerical modeling of their effects on SSI*. PhD thesis. MSSMat CNR UMR 8579 laboratory, CentraleSupélec, Paris-Saclay University, Châtenay-Malabry, France.

[5]   D. Aubry and A. Modaressi (1996): *GEFDyn - manuel scientifique*. Ecole Centrale Paris, France: MSSMat laboratory, July.

[6]   H. Modaressi (1987): *Modélisation numérique de la propagation des ondes dans les milieux poreux anélastiques*. PhD thesis. LMSSMat, Ecole Centrale Paris, Châtenay-Malabry, France.

[7]   O.C. Zienkiewicz and R.L. Taylor (1991): *The Finite element method, solid and fluid mechanics, dynamics and nonlinearity*, volume 2. McGraw-Hill Book Company, London, 4th edition.

[8]   K. Terzaghi (1943): *Theoretical Soil Mechanics*. John Wiley & Sons.

[9]   F. Lopez-Caballero and A. Modaressi (2011): Numerical analysis: Specification and validation of used numerical methods. FP7-SME-2010-1-262161, *PREMISERI project*, Paris, France.

[10]   H. Modaressi and I. Benzenati (1994): Paraxial approximation for poroelastic media. *Soil Dynamics and Earthquake Engineering*, 13(2):117–129.

[11]   D. Aubry, D. Chouvet, A. Modaressi, and H. Modaressi (1985): *GEFDyn 5, logiciel d'analyse du comportement statique et dynamique des sols par elements finis avec prise en compte du couplage sol-eau-air*.

[12]   D. Aubry, J.C. Hujeux, F. Lassoudiere, and Y. Meimon (1982): A double memory model with multiple mechanisms for cyclic soil behavior. In *International Symposium on Numerical Modeling in Geomechanics*, pages 3– 13, Balkema ed.

[13]   J.C. Hujeux (1985): Une loi de comportement pour le chargement cyclique des sols. In *Génie Parasismique*, pages 278–302, France. Presses ENPC. Edited by V. Davidovici.

[14]   F. Lopez-Caballero and A. Modaressi-Farahmand-Razavi (2010): Assessment of variability and uncertainties effects on the seimic response of a liquefiable soil profile. *Soil Dynamics and Earthquake Engineering*, 30(7): 600–613.

[15]   F. Lopez-Caballero, A. Modaressi-Farahmand-Razavi and H. Modaressi (2007): Nonlinear numerical method for earthquake site response analysis i - elastoplastic cyclic model and parameter identification strategy. *Bulletin of Earthquake Engineering*, 5(3): 303–323, June.

[16]   M.B. Darendeli (2001): Development of a new family of normalized modulus reduction and material damping curves. PhD thesis, The University of Texas, Austin, Texas.

[17]   F.J. Vechio and M.B. Emara (1992): Shear deformation in reinforced concrete frames. *ACI Structural journal*, 89(1): 46–56.

[18]   E. Saez, F. Lopez-Caballero, and A. Modaressi-Farahmand-Razavi (2013): Inelastic dynamic soil-structure interaction effects on moment resisting frame buildings. *Engineering structures*, 51(1): 166–177.

[19]   G. Mylonakis and G. Gazetas (2000): Seismic soil-structure interaction: beneficial or detrimental? *Journal of Earthquake Engineering*, 4(3): 277–301.

[20]   M. Shinozuka and K. Ohtomo (1989): Spatial severity of liquefaction. In *Proceedings of the 2nd US-Japan workshop in liquefaction, large ground deformation and their effects on lifelines*, 193–206, New York.

[21]   J. Mitchell, H. Cooke and J. Schaeffer (1998): Design considerations in ground improvement for seismic risk mitigation. In *Geotechnical Earthquake Engineering and Soil Dynamics III*, Editors: Dakoulas, P., Yegian, M., and Holtz, R. D., volume 1, 580–613, Seattle, Washington. ASCE. Geotechnical Special Publication No. 75.